Development of novel cocrystal-based active food packaging by a quality by design approach

DEVELOPMENT OF NOVEL COCRYSTAL-BASED ACTIVE FOOD PACKAGING BY A QUALITY BY DESIGN APPROACH

Federica Bianchi[1,2*], Fabio Fornari[1], Nicolò Riboni[1,3], Costanza Spadini[4], Clotilde Silvia Cabassi[4], Mattia Iannarelli[4], Claudia Carraro[1], Paolo Pio Mazzeo[1], Alessia Bacchi[1,5], Serena Orlandini[6], Sandra Furlanetto[6*], Maria Careri[1,7]

[1]Department of Chemistry, Life Sciences and Environmental Sustainability, University of Parma, Parco Area delle Scienze 17/A, 43124 Parma, Italy

[2]Interdepartmental Center for Packaging (CIPACK), Parco Area delle Scienze, 43124 Parma, Italy

[3]Center for Energy and Environment (CIDEA), Parco Area delle Scienze 42, 43124 Parma, Italy

[4]Department of Veterinary Sciences, University of Parma, Strada del Taglio 10, 43121 Parma, Italy

[5]Biopharmanet-TEC, University of Parma, Parco Area delle Scienze 27/A, 43124 Parma, Italy

[6]Department of Chemistry "U. Schiff", University of Florence, Via U. Schiff 6, 50019 Sesto Fiorentino, Florence, Italy

[7]Interdepartmental Center on Safety, Technologies and Agri-Food Innovation (SITEIA.PARMA), Parco Area delle Scienze, 43124 Parma, Italy

*Corresponding authors:

Federica Bianchi: E-mail: federica.bianchi@unipr.it. Phone: +39 0521 905446.

Sandra Furlanetto: E-mail: sandra.furlanetto@unifi.it. Phone: +39 0554573717.

Abstract

Food waste is a long-standing issue having a strong impact on modern society. A way to reduce food waste can be related to the increase of the shelf-life of food as a result of improving the package type. An innovative active food packaging material based on cocrystallization of microbiologically active compounds present in essential oils was developed following the Quality by Design principles. Carvacrol, thymol and cinnamaldehyde were selected as active components and their concentration optimized to produce plastic films characterized by antimicrobial properties against four bacterial strains involved in fruit and vegetable spoilage. The developed packaging prototypes were characterized in terms of both antimicrobial activity and prolonged release of the active components of essential oils assessing the inhibiting power both by contact and in gas phase. Finally, the prolonged shelf-life of fruit samples stored at room temperature was demonstrated.

Keywords: Quality by design; Cocrystals; Essential oils; Packaging; Shelf-life

1. Introduction

Food waste is an issue of importance to global food security and good environmental governance, having environmental, economic, and social impacts. It has been estimated that in the EU 20% of the total food produced is lost or wasted, while 43 million people cannot afford a quality meal every other day (Stenmarck, Jensen, Quested, & Moates, 2016). A way to reduce food waste and strengthen sustainability of food cycle is the extension of food shelf-life, defined as the period of time during which the quality of the packaged food remains acceptable in terms of organoleptic properties and health safety, maintaining the physical, chemical and biological alterations within acceptable limits (Conte, Cappelletti, Nicoletti, Russo, & Del Nobile, 2015). An interesting approach to prevent food deterioration is the development of active packaging: active materials are designed to embed components able both to release substances into the packaged food and to absorb compounds from the surrounding environment (Commission of the European Communities, 2009). Accordingly, food preservatives such as antimicrobials, moisture scavengers, carbon dioxide emitters and antioxidants can be directly incorporated into the packaging system. The main advantages rely on the possibility to reduce the amount of substances required to be effective compared to their addition in food bulk, as well as to avoid their direct contact with food during processing, which may result in a decrease of their efficacy (Huang, Qian, Wei, & Zhou, 2019; Yildirim et al., 2018). However, it has been demonstrated that synthetic additives used in active packaging could be associated to adverse health effects, such as allergies, intestinal disorders, increased oxidative stress and formation of carcinogenic compounds (Csáki, 2011). Essential oils (EOs) are natural ingredients produced by plants classified as “Generally Recognized As Safe” (GRAS) by the Food and Drug Administration (Food and Drug Administration, 2016). EOs and their active compounds proved to be effective for food preservation due to their antibacterial, antiviral, antifungal and insecticide properties (Bakkali, Averbeck, Averbeck, & Idaomar, 2008; Fumes, Silva, Andrade, Nazario, & Lanças, 2015). Therefore, their use in active packaging arouses interest and integrated EOs/active compounds of EOs packaging systems are considered a potential

78 industrial solution with high-level expectations (Guillard et al., 2018; Ribeiro-Santos, Andrade,
79 Melo, & Sanches-Silva, 2017).
80 Several active compounds of EOs such as eugenol (Requena, Vargas, & Chiralt, 2019; Wieczyńska
81 & Cavoski, 2018), carvacrol (Kurek, Guinault, Voilley, Galić, & Debeaufort, 2014; Wieczyńska &
82 Cavoski, 2018), thymol (Das et al., 2019; Ferreira, Capello, Siqueira, Lago, & Caseli, 2016) and
83 linalool (Aytac, Yildiz, Kayaci-Senirmak, Tekinay, & Uyar, 2017) proved to be effective
84 antimicrobial agents when integrated in packaging systems. One of the main challenge related to the
85 use of EOs or their active compounds is to stabilize them into the solid state, thus overcoming
86 difficulties related both to their physical state since they are mainly liquid at room temperature and
87 to their volatility, which strongly reduces the performances in industrial applications (Wieczyńska
88 & Cavoski, 2018). In order to overcome these limitations, several solutions have been proposed: i)
89 use of separate carriers containing EOs active component-loaded porous matrices (Otoni, Espitia,
90 Avena-Bustillos, & McHugh, 2016; Wieczyńska & Cavoski, 2018); ii) encapsulation of EOs in
91 chitosan (Kurek et al., 2014; Wu et al., 2019); iii) incorporation of EOs in cyclodextrins (Das et al.,
92 2019; Marques et al., 2019).
93 Cocrystallization is another worthwhile approach to stabilize and to modulate the physical-chemical
94 properties of both EOs and their active components. Cocrystals are crystalline materials composed
95 by active ingredient and suitable coformer bound by weak intermolecular interactions, such as
96 hydrogen bonds, π-π stacking, halogen bonds with definite stoichiometry. Cocrystals generally
97 enhance the dissolution rate and solubility of pure active ingredients, have higher melting points
98 than those of either of the pure components and alter the release profile of pure essential oils
99 (Aakeröy & Salmon, 2005; Mazzeo et al., 2019).
100 In a research program dealing with the study of properties of cocrystals as a function of pairing EOs
101 each with a different conformer, the aim of the study was to evaluate the capabilities of EO-based
102 cocrystals having carvacrol, eugenol, thymol and cinnamaldehyde as active components to produce
103 plastic films characterized by antimicrobial properties against four reference bacterial strains. New

cocrystals were synthetized to tune the oil release profile: for this purpose, a Quality by Design (QbD) strategy (Food and Drug Administration, 2004; ICH Harmonised Tripartite Guideline, 2009) was used to assure the quality of the final product measured in terms of its performance to inhibit synergistically selected microorganisms commonly involved in fruit and vegetable deterioration. For the first time in the literature a risk-based and systematic approach was applied to food packaging materials development, making possible to assure the quality of the product. Finally, the results were compared with those of the pure EOs.

2. Material and Methods

2.1. Chemicals, culture media and bacterial strains

Dimethyl sulfoxide, acetone (both > 99.5 % purity), chitosan (310–375 kDa), isonicotinamide (INA), cinnamaldehyde (CIN), glacial acetic acid and NaOH (all > 99% purity) were purchased from Sigma-Aldrich (Milan, Italy); methanol (> 99.8% purity), thymol (THY) and 4-hydroxybenzoic acid (4HBA) (both > 99% purity) were purchased from Honeywell (Seelze, Germany); carvacrol (CAR), eugenol (EUG) and hexamethylenetetramine (HMT) (all > 99% purity) were from Carlo Erba (Milan, Italy); N,N′-dimethylformamide (DMF, 99.8% purity) was purchased from VWR International (Milan, Italy).

Mueller Hinton broth, Mueller Hinton agar, MacConkey agar and phosphate buffer (pH 7) were purchased from Biolife (Milan, Italy).

Microbiological assays were carried out on *Escherichia coli* ATCC 25922, *Salmonella Typhimurium* ATCC 14028, *Staphylococcus aureus* ATCC 25923, and methicillin-resistant (MR) *Staphylococcus aureus* ATCC 43300 reference strains.

2.2. Synthesis of cocrystals

All cocrystals were prepared in bulk by grinding or direct mixing methods without adding any further solvent. HMT-THY cocrystal was synthetized according to a previous published procedure

(Mazzeo et al., 2019). Isonicotinamide-carvacrol (INA-CAR) cocrystal was prepared by adding 122.0 mg isonicotinamide (1 mmol) to 153 µl carvacrol (1 mmol) in a ceramic mortar. The mixture phase was ground with a pestle under fume hood aspiration for 10 minutes until a whitish homogeneous phase was obtained.

4-hydroxybenzoic acid-cinnamaldehyde (4HBA-CIN) cocrystal was synthetized by adding 138.0 mg 4-hydroxybenzoic acid (1 mmol) to 126 µl cinnamaldehyde (1 mmol) in a ceramic mortar. The mixture thus obtained was ground with a pestle under fume hood aspiration for 10 minutes until a whitish homogeneous phase was gathered.

The purity of the samples was assessed by PXRD (Powder X-Ray Diffraction) by using a ARL X'TRA diffractometer (Thermo Fisher Scientific, MA, USA) in theta−theta Bragg−Brentano geometry with CuKα radiation. The thermal stability of the compounds was checked by DSC (Differential Scanning Calorimetry) analyses using a PerkinElmer Diamond instrument (PerkinElmer, Waltham, MA, USA) equipped with a model ULSP 90 ultracooler, in closed 50 µL Al-pans at 5 °C/min. The crystal structure of INA-CAR and 4HBA-CIN were determined by single crystal X-ray diffraction. Single crystals of the two cocrystals were obtained by crystallization from DMF and acetone, respectively, and mounted on a SMART APEX2 diffractometer (Bruker, Billerica, MA. USA). Data were collected at low temperature using MoKα radiation (λ= 0.71073 Å); Lorentz polarization and absorption correction were applied by using APEX v3 software. Structures were solved by direct methods using SHELXT35 and refined by full-matrix leasts-squares on all F^2 using SHELXL36 implemented in Olex2.21.37. All non-H atoms were refined anisotropically. Hydrogen atoms were introduced in calculated positions. Details on the software used are in the Supplementary material. Crystallographic data have been deposited with the Cambridge Crystallographic Data Centre as supplementary publications nos. CCDC 2014876-2014877. Copies of the data can be obtained free of charge on application to CCDC, 12 Union Road, Cambridge CB2 1EZ, UK (fax: (+44) 1223-336-033; e-mail: deposit@ccdc.cam.ac.uk.

156 2.3. Antimicrobial activity of the active components of EOs

157 2.3.1. Inoculum preparation

158 Five bacterial colonies from solid fresh cultures of each tested strain were inoculated in sterile tubes
159 with Mueller Hinton broth and incubated at 37°C for 24 h. After incubation, the bacterial
160 suspension was centrifuged at 2000 rpm at 4°C for 20 minutes in order to separate the bacterial
161 pellet from the supernatant. Then, the pellet was resuspended in phosphate buffer (PB) 10 mM pH
162 7. The bacterial suspension was adjusted in PB to obtain an optical density (OD) value at 600 nm in
163 a 1 cm light path cuvette in the range 0.08–0.13, approximately equivalent to a 10^8 CFU/mL (CFU:
164 colony-forming unit) suspension. This suspension was further diluted 1:100 in sterile Mueller
165 Hinton broth. Fifty µL of the bacterial suspension containing 10^6 CFU/mL were inoculated into
166 each well to obtain a final concentration of $5 \cdot 10^5$ CFU/mL. Bacterial suspensions were investigated
167 with the aid of a Biophotometer plus (Eppendorf, Hamburg, Germany) spectrophotometer (λ = 600
168 nm).

169 All the microbiological assays were performed within 30 min after the inoculum standardization.

170

171 2.3.2. Minimal inhibitory concentration (MIC) assay

172 MIC assay was evaluated according to the CLSI guidelines (CLSI, 2018) by following the protocol
173 proposed by Wiegand et al. (Wiegand, Hilpert, & Hancock, 2008), with minor modifications.
174 Diluted stock solutions were obtained in sterile Müller Hinton broth. Fifty µL of the serial two-fold
175 dilutions 2–1024 µg/mL range of the stock solution were added into a 96-well microtiter plate
176 (Greiner, Milan, Italy). Thereafter, 50 µL of the bacterial suspension containing 10^6 CFU/mL were
177 added in each well to obtain a concentration of $5 \cdot 10^5$ CFU/mL. Growth and sterility controls were
178 performed for each bacterial strain.

179 Plates were incubated for 24 h at 37°C in aerobic atmosphere. The minimal inhibitory concentration
180 is the lowest concentration of the tested compound at which there was no visible growth. Each
181 assay was repeated independently nine times.

182

183 2.3.3. Time-kill assay (TKA)

184 The antimicrobial activity was also evaluated as a function of time with TKA (NCCLS, 1999). In a
185 96-well microtiter plate (Greiner) 100 µL of adjusted bacterial suspension with a final bacterial
186 concentration of $5 \cdot 10^5$ CFU/mL and an equal volume of a solution containing the tested
187 antimicrobial compound were used so that the final concentration of the tested compound was equal
188 to its MIC. Growth and sterility controls were performed for each bacterial strain. Microtiter plates
189 were incubated at 37°C in aerobic atmosphere. After 0, 2, 4, 6, 8 and 24 hours of contact, 20 µL of
190 the suspension were plated on solid agar medium (Mueller Hinton agar for Gram-positive strains
191 and MacConkey agar for Gram-negative strains) and incubated for 24 h at 37°C in aerobic
192 atmosphere. After incubation CFU were counted. Each assay was independently replicated three
193 times.

194 Inhibition percentages ($I_{\%}$) were calculated as follows:

$$I_{\%} = \left(1 - \frac{N_i^t}{N_{GC}^t}\right) \times 100$$

195 where N_i^t represents CFU counted in the i^{th} experiment at a given time t and N_{GC}^t represents CFU
196 counted in the growth control experiment at the same time t.

197

198 2.4 Quality by Design

199 The Quality Target Product Profile (QTTP) was defined as the synergistic inhibition towards the
200 selected strains considering a threshold value of 0.05 au, corresponding to the absence of visible
201 microbial growth. The Critical Process Parameters (CPPs) were cinnamaldehyde, thymol and
202 carvacrol concentrations. The knowledge space was defined by the CPPs investigated in the 40–150
203 µg/mL range.

204 The Critical Quality Attributes (CQAs), able to measure the product quality, were the absorbance
205 values of each bacterial suspension registered by means of a Multiskan FC Microplate Photometer

206 (Thermo Fisher Scientific) (λ = 620 nm) after 24 h incubation at 37°C in aerobic atmosphere.
207 Multilinear regression was used to correlate CPPs with each CQA: a Box-Wilson central composite
208 face-centered design (CCF) was used to estimate the model coefficients.
209 Each CPP was studied at three levels for a total of 2^k+2k+n_0 runs, where k = 3 was the number of
210 factors and n_0 = 6 was the number of the experiments at the center of the experimental domain for
211 the estimation of the experimental variance. All the other experiments were independently
212 replicated three times, thus obtaining an experimental plan composed by 48 runs. All the
213 experiments were carried out in a 96-well microtiter plate using Mueller Hinton broth with a
214 bacterial concentration in each well equal to $5 \cdot 10^5$ CFU/mL.
215 Analysis of Variance (ANOVA) was applied in order to assess the significance of the obtained
216 regression models. For defining the design space (DS), Monte-Carlo simulations (Herrador, Asuero,
217 & González, 2005) were carried out in order to propagate the predictive error by using the model
218 equation to the CQAs, so that the probability of reaching the desired objective was computed and
219 shown as probability surfaces. The DS was established for a specified quality level ≥ 95%. Finally,
220 the DS was validated by performing experiments at its edges, selected by a Plackett-Burman design
221 in which the -1 and +1 levels corresponded to the extremes of the DS interval for each CPP, and
222 verifying the fulfilment of the requirements. The experiments were replicated three times for each
223 strain and the Dong's algorithm (Dong, 1993) was used to assess the significance of the CPPs.
224
225 2.5. Food packaging material
226 2.5.1. Preparation
227 Packaging prototypes were realized by adhesion of cocrystals on low density polyethylene (LDPE)
228 using chitosan: 50 μL of a chitosan solution (Petriccione et al., 2015) were pipetted on LDPE
229 supports and air-dried for 1 h at room temperature, then proper amounts of cocrystals were
230 anchored to the plastic support by dispersing the cocrystals onto the chitosan film.
231

232 2.5.2. Antimicrobial activity of packaging material

233 The antimicrobial activity of the food packaging was evaluated both by contact and in the vapor
234 phase using a mixture of all the bacterial strains at the overall concentration of $5 \cdot 10^5$ CFU/mL.
235 Before use, packaging prototypes were sterilized under UV light for 1 h. The antimicrobial activity
236 in the vapor phase was assessed by means of the disc volatilization method (Tyagi & Malik, 2011),
237 whereas the antimicrobial effect exerted by contact was evaluated by immersing the packaging
238 prototypes in 15 mL of inoculated Mueller Hinton broth in sterile tubes. After incubation at 37°C
239 for 24 h, 100 µL of broth were pipetted into a 96-well microtiter plate and the absorbance was
240 measured by means of a Multiskan FC Microplate Photometer at λ = 620 nm. Growth and sterility
241 controls were also planned. Inhibition percentages ($I_{\%}$) were calculated as follows:

$$I_{\%} = \left(1 - \frac{A_i^{620nm} - A_{SC}^{620nm}}{A_{GC}^{620nm} - A_{SC}^{620nm}}\right) \times 100$$

242 where A_i^{620nm} represents the absorbance registered for the i^{th} experiment, A_{SC}^{620nm} represents the
243 absorbance registered for the sterility control experiment and A_{GC}^{620nm} represents the absorbance
244 registered for the growth control experiment.

245

246 2.5.3. Release of active compounds of EOs

247 Packaging prototypes were inserted into 10 mL glass vials and maintained at room temperature for
248 14 days.

249 Headspace GC-MS analyses were carried out by injecting 1 mL of the headspace above the sample
250 into the gas chromatograph by using a PAL COMBI-xt autosampler (CTC Analytics AG, Zwingen,
251 Switzerland). A HP 6890 Series Plus gas chromatograph (Agilent Technologies, Palo Alto, CA,
252 USA) equipped with an MSD 5973 mass spectrometer (Agilent Technologies) was used. The carrier
253 gas was helium at a constant flow of 1.3 mL/min. The injection port was held at 270°C and the
254 injection was carried out in split mode (split ratio 10:1). Chromatographic separation was performed
255 on a 30 m × 0.25 mm, df 0.25 µm Rxi-17Sil MS capillary column (Restek, Bellafonte, USA) using

256 the following temperature program: initial temperature 70°C, 10°C/min up to 140°C, 5°C/min up to
257 170°C. The transfer line and source were maintained at the temperatures of 270 and 150°C,
258 respectively. Full scan electron ionization (EI) data were acquired under the following conditions:
259 ionization energy: 70 eV; mass range: 40−200 amu; scan time: 3 scan/s; electron multiplier voltage:
260 1953 V. Signal acquisition and data handling were performed using the HP Chemstation software
261 (Agilent Technologies). Three independent replicated measurements were always performed.
262
263 2.6. Application to fresh fruit
264 White grapes (variety: Vittoria) was used as model fruit to assess the reliability of the packaging
265 prototypes
266 2.6.1. Microbiological assessment
267 Microbiological assessment of grapes in contact with packaging prototypes was performed
268 according to the UNI EN ISO 4833-1:2013 to determine the total mesophilic count in foods [UNI
269 EN ISO 4833-1:2013].
270 The total mesophilic count of treated and untreated grapes (control) was evaluated at different
271 times: i) within 1 h of contact with the packaging prototypes), ii) after 3 days of contact and iii)
272 after 7 days of contact by maintaining the fruit at room temperature into glass containers with a
273 perforated cap.
274
275 2.6.2. Sensory evaluation
276 Sensory analysis was performed in order to evaluate the effect of the developed prototypes on the
277 organoleptic properties of grapes stored at room temperature for a period of 7 days. Not
278 functionalized LDPE was used as control: four main features were investigated, namely appearance
279 (color uniformity and presence, dimensions and numbers of strains eventually present onto the
280 cherry skin), texture (fruit turgidity and pulp texture), flavor and taste. The sensory analysis was
281 performed by a panel of 10 untrained panellists (4 males and 6 females). The analysis was

282 performed by evaluating the described attributes using an intensity scale from 0 to 10, where 10
283 indicates the top-level features. Grapes evaluation was performed by each panellist blindly
284 evaluating 3 grapes *per* group. Samples were coded and judged in random order to avoid bias.
285 Finally, mean grades and standard deviations for each attribute were computed.
286
287 2.6. Statistical analysis
288 Data analyses were performed using MODDE v.10 software (MKS Umetrics AB, Umeå, Sweden),
289 and SPSS Statistics v.23.0 (IBM, Milan, Italy) statistical packages.
290
291 **3. Results and discussion**
292 In this study cocrystallization is proposed to extend the use of natural products for packaging
293 applications: in the case of active components of EOs, cocrystallization generally increases the
294 melting point of the material and induces the stabilization of a liquid ingredient in a solid form
295 (Bacchi et al., 2016). This is a really important matter since liquid or low melting point compounds
296 are not useful for industrial applications. Our attention was focused on active components of EOs
297 which are mainly liquid at room temperature, hence there is the need to stabilize them into the solid
298 state form to produce plastic films having antimicrobial properties.
299
300 3.1. Minimal inhibitory concentration assay and Time-kill assay
301 In order to select the most suitable active components of EOs to be used for cocrystallization,
302 preliminary experiments were carried out in terms of MIC assay and time-kill assay. The effects of
303 EUG, CIN, THY, and CAR were tested on a pool of microorganisms commonly found in
304 vegetables and fruit (European Commission, 2002) like Gram-negative bacteria, i.e. *Escherichia*
305 *coli* and *Salmonella Typhimurium*, and Gram-positive bacteria, i.e. *Staphylococcus aureus*, and MR
306 *Staphylococcus aureus*. EUG was discarded owing to its poor inhibiting power (MIC value of 1024
307 μg/mL and greater) (Table 1); as for the other active components of EOs, a different behavior

toward each strain was observed (Fig. 1). It has to be considered that bactericidal effect is exerted only when an antimicrobial compound is able to kill bacteria in percentage higher than 99.9%, whereas bacteriostatic behavior means that the active compound is capable to prevent the microbial growth. The achieved results proved that CIN was able to exert a bacteriostatic effect within 6 h, THY a bactericidal effect within 2 h, whereas CAR exerted both a bactericidal effect on Gram-negative and a bacteriostatic effect on Gram-positive microorganisms. These findings demonstrated that only a mixture of active compounds of EOs can be effective to obtain the simultaneous inhibition of all the microorganisms.

The approach commonly used in microbiology for assessing the inhibiting effect toward target microorganisms is the so-called checkerboard assay (Meletiadis, Pournaras, Roilides, & Walsh, 2010), in which two components at a time are combined with proper concentration values within an established range. Despite this procedure allows for the calculation of the fractional inhibitory concentration index, it is time-consuming and requires a lot of experiments to evaluate the interactions between more than two compounds. Since data deriving from TKA revealed that the required broad antimicrobial effect could be achieved only by using a mixture of the three investigated active components, a QbD approach was used to optimize the simultaneous inhibition of the selected microorganisms.

3.2. Quality by Design

Preliminary experiments were carried out in order to select the experimental range in which the CPPs, i.e. the concentration of CIN (x_1), THY (x_2) and CAR (x_3) had to be varied: briefly, it was observed that the combination of cinnamaldehyde, thymol and carvacrol at concentration values lower than 40 μg/mL each did not produce inhibition towards the investigated microorganisms, whereas their use at 150 μg/mL each provided almost 99% inhibition towards all the strains. Hence, the selected range for each CPP was 40-150 μg/mL.

A CCF was applied for estimating the coefficients of the quadratic models relating the CPPs to selected CQAs. ANOVA showed that all the calculated models were significant ($p < 0.05$) with $R^2 > 0.8$ and valid $Q^2 > 0.7$, thus highlighting the goodness of fit and the predictive capability in cross-validation. As shown in Table S1, the performance of the models including reproducibility values confirmed that the models could be used for the subsequent studies, investigating coefficients and contour plots.

Fig. 2 shows the contour plots obtained by setting CIN at the medium level, namely 95 μg/mL, and representing the response as a function of THY and CAR. From these plots it is possible to note that, even if some differences in the trends were observed for the four microorganisms, the higher inhibition, corresponding to the lower absorbance values, was in general achieved at high levels for CAR and medium-high levels for THY.

To consider all the four CQAs simultaneously considering all the four CQAs and for to better pointing out the region which provided the best results, a desired threshold value of 0.05 au, corresponding to an average inhibition of 92 (±3) % (n = 10), was set as an acceptable maximum for each CQA. By using desirability function, the sweet spot plots depicted in Fig. S1, maintaining CIN at the medium level, were obtained. The different colors refer to the zones where the desired value of au target was achieved for one or more predicted CQAs. In particular, the sweet spot, namely the optimal zone where all the four requirements were fulfilled, is depicted in bright green.

For calculating the design space, the concept of probability that the desired performances are met was considered (Orlandini, Pinzauti, & Furlanetto, 2013). A target desired value of 0.04 au and a target accepted value of 0.05 au were set for each CQA in order to assure a satisfactory inhibition of the microorganisms. A set-point was selected within the sweet spot region, corresponding to 105 μg/mL CIN, 116 μg/mL THY and 141 μg/mL for CAR, respectively. Monte-Carlo simulations were used for expanding factor ranges from this point to the largest possible range where all the predicted CQAs fulfill the requirements and for drawing the probability maps. These maps show how the

CPPs settings could be varied around the selected set-point still guaranteeing a level of probability ≥ 95% that the CQAs limits are not exceeded.

The design space was graphically represented as the green zone in the probability map reported in Fig. 3, drawn maintaining CIN at 105 μg/mL, and resulted to be enclosed within the following intervals: 84−126 μg/mL for CIN; 93−138 μg/mL for THY and 125−150 μg/mL for CAR.

The DS was validated by a Plackett-Burman design and the obtained results showed that in every verification point the complete inhibition of all the considered bacteria was achieved.

Hence, the combination of the values of all the CPPs within the DS allowed the inhibition of all the considered microorganisms by maintaining the overall antimicrobial concentration below the highest MIC value needed for each active component of EOs, with the additional advantage to exert inhibition toward all considered strains.

3.3. Cocrystals-based packaging material

3.3.1. Cocrystals synthesis and antimicrobial properties

On the basis of the achieved results, different cocrystals were synthetized. The coformers used for cocrystallization were selected among the harmless compounds used as food additives ("Regulation (EC) No 1333/2008 of the European Parliament and of the Council of 16 December 2008 on food additives," 2008), focusing on HMT and 4HBA. HMT is a food preservative used in cheese, it has no antimicrobial action on its own, but its antimicrobial effect is related to the release of formaldehyde in an acidic medium, thus requiring the subsequent quantitation of formaldehyde content in terms of migration. 4HBA is mostly applied in food industry as flavoring and antioxidant agent, or as intermediate for food preservatives. INA, an isomer of nicotinamide, one of the forms of the hydrosoluble vitamin complex B3, commonly used in the pharmaceutical industry as a conformer with active ingredients in drug formulations, was also tested (Reddy, Babu, & Nangia, 2006). The thermal stability and the purity of powders obtained were checked with solid-state techniques such as DSC and PXRD analysis (Fig. S2-S5). While the crystal structure of HMT-THY

has recently been determined (Mazzeo et al., 2019), those of INA-CAR and 4HBA-CIN were determined in this study. Crystal data and structure determination results are reported in Table S2. The intermolecular interactions observed explain the stabilization of the volatile ingredients within the solid. INA-CAR crystallizes in a 1:1 molar ratio and the expected hydroxyl···pyridine hydrogen bond is observed between the two molecular partners (N···O = 2.757(2) Å) (Fig. S6), whereas the amide groups of INA are hydrogen bonded each other in an N-H···O homosynthon (N···O = 2.948(3) Å) (Fig. S7). This interaction creates a hydrogen-bonded chain of four molecules terminated by EO molecules which sandwich two molecules of isonicotinamide. The interaction between the hydroxyl group of CAR and the amide of INA (N···O = 3.265(3) Å) coordinates each array of four molecules. 4HBA-CIN crystallizes in a 1:1 molar ratio (Fig. S6). 4-hydroxybenzoic acid is engaged in a hydrogen bond between its hydroxyl group and the carbonyl group of CIN (O···O = 2.691(2) Å) (Fig. S8). Similarly, the acidic group of 4HBA forms the homomeric head-to-head association (O···O = 2.622(2) Å) creating a hydrogen-bonded chain of four molecules along the crystallographic ***b*** axis (Fig. S9). All the selected coformers were preliminary tested in terms of MIC: values higher than 1024 μg/mL were always obtained, thus proving the absence of inhibition capability of coformers alone toward the investigated microorganisms.

Finally, the antimicrobial activity of the cocrystals was evaluated in terms of MIC considering the stoichiometric ratio between the active components of EOs and each conformer, obtaining MIC values in agreement with those achieved in the case of the active components of EOs (Table S3).

Taking into account that our previous study (Mazzeo et al., 2019) demonstrated that cocrystallization is able to reduce the release of the volatile compounds in the gas phase, thus guaranteeing the availability of the active compounds for a longer time, prototypes of plastic packaging were prepared and characterized in terms of microbiological activity.

3.3.2. Packaging prototypes

409 Since the obtained cocrystals were characterized by melting points lower than 100°C, they were not
410 suitable for the extrusion process (Table 2). Therefore, a different strategy based on the adhesion of
411 cocrystals on the surface of the plastic material, namely LDPE, was selected. Chitosan was chosen
412 as a suitable substrate for cocrystal adhesion because of its non-toxicity and its proven antimicrobial
413 properties (Bellich, D'Agostino, Semeraro, Gamini, & Cesàro, 2016). The proper amount of
414 cocrystals to be anchored on the plastic film was established taking into account both the optimized
415 concentrations of CIN, THY and CAR obtained by the QbD approach, and the stochiometric ratio
416 between the active components of the EOs and the coformer in the cocrystals.
417 Taking into consideration that volatile substances such as active compounds of EOs can exert
418 inhibition both by contact and in the vapor phase (López, Sánchez, Batlle, & Nerín, 2005; Tyagi &
419 Malik, 2011), the antimicrobial activity of the crystalline packaging was tested by applying both
420 strategies. A broad inhibition zone with an average diameter of 32 (±6) mm (n = 4) was observed in
421 the case of the evaluation of the antimicrobial activity in the gas phase (Fig. S10).
422 As for the assessment of the antimicrobial activity by contact, since it is known that chitosan could
423 be able to exert antimicrobial activity, additional experiments were performed to compare the
424 inhibition capability of chitosan-coated LDPE vs cocrystals-based LDPE. The achieved results
425 proved that the active crystalline packaging had a superior inhibiting power if compared to the
426 chitosan-coated LDPE ($p < 0.05$) with an outstanding effect size (Cohen's $d > 2.0$, n = 4 for each
427 material). In particular, the addition of cocrystals proved to be effective in enhancing the inhibition
428 capability towards the microorganisms with a factor 3 with respect to the chitosan-coated
429 packaging.
430 An additional advantage of the proposed prototypes relies on the slow release of the active
431 components of EOs along the time. In fact, as depicted in Fig. 4 and as highlighted by ANOVA, the
432 amount of active components released from the packaging prototype in the vapor phase remained
433 constant ($p > 0.05$, n = 3) for all the duration of the experiment (14 days).
434

435 3.4. Shelf-life evaluation of grape samples

436 3.4.1. Microbiological analysis

437 Regarding the determination of the total mesophilic count, no significant difference between the
438 CFU was observed within 1 h of contact ($p > 0.05$, n = 3). After 3 days of contact, treated grapes
439 showed an inhibition higher than 86% compared to the control. The same behavior was observed
440 after 7 days of contact, thus demonstrating that the proposed prototypes are able to exert
441 antimicrobial activity on real samples (Fig. S11).

442

443 3.4.2. Sensory evaluation

444 Appearance, texture, flavor, and taste of white grapes packed in non-functionalized LDPE (control)
445 and in the developed active prototypes were evaluated. The average grades for each attribute are
446 depicted in the radar plots shown in Fig. S12. As shown in the Figure, the use of the antimicrobial
447 packaging resulted in no significant difference for texture and taste compared to the control samples
448 for days 0 and 1, respectively. Regarding appearance, a slight yellowing was observed after 24
449 hours of contact, however, starting from day 3 significantly higher grades were assigned to the
450 antimicrobial-packed grapes. In particular, the presence of stains, skin matting and mold were
451 observed in the control grapes, until an almost complete rotting of the fruit after 7 days. After 24h, a
452 softening of the pulp occurred in the control samples and by day 5, grapes lost their texture. As for
453 the flavor, the use of the cocrystal-based packaging resulted in the presence of a strong, but not
454 unpleasant odor. Therefore, the grade assigned to grapes for the first three days was lower or not
455 significantly different compared to the control. Starting from day 3 a foul smell was perceived in
456 grapes control, and after 5 days the rotten smell was dominant. Obviously, under these conditions
457 grapes were not tasted. By contrast, the mean grades achieved using the developed prototypes were
458 not significantly different from the first to the seventh day ($p > 0.05$), thus suggesting that the
459 developed pack can be able to increase product shelf-life.

460

Conclusions

A Quality by Design approach was applied for the first time to develop an antimicrobial packaging based on the use of active compounds of EOs against bacterial strains involved in fruit and vegetable spoilage. This strategy was crucial to achieve the simultaneous inhibition of the investigated microorganisms, thus allowing the optimization of the concentrations of the active components in the pack formulation. Cocrystallization proved to be a powerful tool to obtain the prolonged release of the active compounds of EOs for a minimum of 14 days. The antimicrobial activity of the developed prototypes was assessed both by contact and in gas phase. The achieved results demonstrated the superior efficacy of the proposed pack in regulating the growth of the investigated strains both with and without the need of a direct contact with the culture medium, with inhibition percentages up to 69 (±15)% (n = 4) evaluated by contact. Reliability of the developed material was also demonstrated by storing fresh fruit, obtaining both the improvement of the organoleptic properties and the reduction of the total microbial charge. This study can be considered the first step towards the development of cocrystalline active packaging based on the use of active components of EOs: the achieved results demonstrate that this approach can be considered a promising tool for shelf-life prolongation of foodstuff. An open challenge for scientific research will be the development of new cocrystals characterized by enhanced thermal stability to be used for pack extrusion, thus facilitating the industrial scale-up.

Acknowledgments

This work was supported by the Italian Ministry of Agricultural, Food, Forestry Policies and Tourism (MIPAAFT)-project PAC/Packaging Attivo Cristallino.

This work has also benefited from the framework of the COMP-HUB Initiative, funded by the 'Departments of Excellence' program of the Italian Ministry for Education, University and Research (MIUR, 2018-2022).

Author Contributions

Conceptualization: F.B; Data curation: CS.C., PP.M., N.R.; Formal analysis: C.S., F.F., C.C., PP.M., N.R.; Funding acquisition: A.B.; Investigation: C.S., F.F., C.C., PP.M., M.I.; Methodology: F.B., S.O.; Resources: F.B., M.C., A.B.; Supervision: F.B., CS.C., A.B.; Validation: F.F.; Roles/Writing - original draft: F.B., F.F., N.R., S.O., C.C. Writing - review & editing: F.B., S.F., M.C, A.B., S.O. CS.C.

Declaration of Competing Interest

The authors declare that they have no known competing financial interests or personal relationships that could have appeared to influence the work reported in this paper.

References

Aakeröy, C. B., & Salmon, D. J. (2005). Building co-crystals with molecular sense and supramolecular sensibility. *CrystEngComm*, *7*, 439–448. https://doi.org/10.1039/b505883j

Aytac, Z., Yildiz, Z. I., Kayaci-Senirmak, F., Tekinay, T., & Uyar, T. (2017). Electrospinning of cyclodextrin/linalool-inclusion complex nanofibers: Fast-dissolving nanofibrous web with prolonged release and antibacterial activity. *Food Chemistry*, *231*, 192–201. https://doi.org/10.1016/j.foodchem.2017.03.113

Bacchi, A., Capucci, D., Giannetto, M., Mattarozzi, M., Pelagatti, P., Rodriguez-Hornedo, N., … Sala, A. (2016). Turning Liquid Propofol into Solid (without Freezing It): Thermodynamic Characterization of Pharmaceutical Cocrystals Built with a Liquid Drug. *Crystal Growth and Design*, *16*, 6547–6555. https://doi.org/10.1021/acs.cgd.6b01241

Bakkali, F., Averbeck, S., Averbeck, D., & Idaomar, M. (2008). Biological effects of essential oils - A review. *Food and Chemical Toxicology*, *46*, 446–475. https://doi.org/10.1016/j.fct.2007.09.106

Bellich, B., D'Agostino, I., Semeraro, S., Gamini, A., & Cesàro, A. (2016). "The good, the bad and the ugly" of chitosans. *Marine Drugs*, *14*, 99. https://doi.org/10.3390/md14050099

CLSI. (2018). Performance Standards for Antimicrobial Susceptibility Testing; In *Clinical and Laboratory Standards Institute* (Vol. 32).

Commission of the European Communities. (2009). Commission Regulation (EU) No 450/2009. *Official Journal of European Union*, (L 135), 3–11.

Conte, A., Cappelletti, G. M., Nicoletti, G. M., Russo, C., & Del Nobile, M. A. (2015). Environmental implications of food loss probability in packaging design. *Food Research International*, *78*, 11–17. https://doi.org/10.1016/j.foodres.2015.11.015

Csáki, K. F. (2011). Synthetic surfactant food additives can cause intestinal barrier dysfunction. *Medical Hypotheses*, *76*, 676–681. https://doi.org/10.1016/j.mehy.2011.01.030

Das, S., Gazdag, Z., Szente, L., Meggyes, M., Horváth, G., Lemli, B., … Kőszegi, T. (2019).

523 Antioxidant and antimicrobial properties of randomly methylated β cyclodextrin – captured
524 essential oils. *Food Chemistry*, *278*, 305–313. https://doi.org/10.1016/j.foodchem.2018.11.047
525 Dong, F. (1993). On the identification of active constrasts in unreplicated fractional factorials.
526 *Statistica Sinca*, *3*, 209–217.
527 European Commission. (2002). Risk Profile on the Microbiological Contamination of Fruits and
528 Vegetables Eaten Raw. In *Report of the Scientific Committee on Food*. Retrieved from
529 https://ec.europa.eu/food/sites/food/files/safety/docs/sci-com_scf_out125_en.pdf
530 Ferreira, J. V. N., Capello, T. M., Siqueira, L. J. A., Lago, J. H. G., & Caseli, L. (2016). Mechanism
531 of Action of Thymol on Cell Membranes Investigated through Lipid Langmuir Monolayers at
532 the Air-Water Interface and Molecular Simulation. *Langmuir*, *32*, 3234–3241.
533 https://doi.org/10.1021/acs.langmuir.6b00600
534 Food and Drug Administration. (2004). *Guidance for Industry PAT - A Framework for Innovative*
535 *Pharmaceutical Development, manufacturing, and Quality Assurance*. Retrieved from
536 https://www.fda.gov/media/71012/download
537 Food and Drug Administration. (2016). *54960 Federal Register / Vol . 81 , No . 159 / Wednesday ,*
538 *August 17 , 2016 / Rules and Regulations*. *81*, 54960–55055.
539 Fumes, B. H., Silva, M. R., Andrade, F. N., Nazario, C. E. D., & Lanças, F. M. (2015). Recent
540 advances and future trends in new materials for sample preparation. *TrAC - Trends in*
541 *Analytical Chemistry*, *71*, 9–25. https://doi.org/10.1016/j.trac.2015.04.011
542 Guillard, V., Gaucel, S., Fornaciari, C., Angellier-Coussy, H., Buche, P., & Gontard, N. (2018). The
543 Next Generation of Sustainable Food Packaging to Preserve Our Environment in a Circular
544 Economy Context. *Frontiers in Nutrition*, *5*, 1–13. https://doi.org/10.3389/fnut.2018.00121
545 Herrador, M. Á., Asuero, A. G., & González, A. G. (2005). Estimation of the uncertainty of indirect
546 measurements from the propagation of distributions by using the Monte-Carlo method: An
547 overview. *Chemometrics and Intelligent Laboratory Systems*, *79*, 115–122.
548 https://doi.org/10.1016/j.chemolab.2005.04.010

549 Huang, T., Qian, Y., Wei, J., & Zhou, C. (2019). Polymeric Antimicrobial Food Packaging and Its
550 Applications. *Polymers*, *11*, 560. https://doi.org/10.3390/polym11030560
551 ICH Harmonised Tripartite Guideline. (2009). ICH Harmonised Tripartite Guideline,
552 Pharmaceutical Development Q8(R2). In *International Council for Harmonisation of*
553 *Technical Requirements for Pharmaceuticals for Human Use*.
554 Kurek, M., Guinault, A., Voilley, A., Galić, K., & Debeaufort, F. (2014). Effect of relative humidity
555 on carvacrol release and permeation properties of chitosan based films and coatings. *Food*
556 *Chemistry*, *144*, 9–17. https://doi.org/10.1016/j.foodchem.2012.11.132
557 López, P., Sánchez, C., Batlle, R., & Nerín, C. (2005). Solid- and vapor-phase antimicrobial
558 activities of six essential oils: Susceptibility of selected foodborne bacterial and fungal strains.
559 *Journal of Agricultural and Food Chemistry*, *53*, 6939–6946.
560 https://doi.org/10.1021/jf050709v
561 Marques, C. S., Carvalho, S. G., Bertoli, L. D., Villanova, J. C. O., Pinheiro, P. F., dos Santos, D.
562 C. M., … Bernardes, P. C. (2019). β-Cyclodextrin inclusion complexes with essential oils:
563 Obtention, characterization, antimicrobial activity and potential application for food
564 preservative sachets. *Food Research International*, *119*, 499–509.
565 https://doi.org/10.1016/j.foodres.2019.01.016
566 Mazzeo, P. P., Carraro, C., Monica, A., Capucci, D., Pelagatti, P., Bianchi, F., … Bacchi, A.
567 (2019). Designing a Palette of Cocrystals Based on Essential Oil Constituents for Agricultural
568 Applications. *ACS Sustainable Chemistry & Engineering*, *7*, 17929–17940.
569 https://doi.org/10.1021/acssuschemeng.9b04576
570 Meletiadis, J., Pournaras, S., Roilides, E., & Walsh, T. J. (2010). Defining fractional inhibitory
571 concentration index cutoffs for additive interactions based on self-drug additive combinations,
572 Monte Carlo simulation analysis, and in vitro-in vivo correlation data for antifungal drug
573 combinations against Aspergillus fumigatus. *Antimicrobial Agents and Chemotherapy*, *54*,
574 602–609. https://doi.org/10.1128/AAC.00999-09

575 NCCLS. (1999). *Methods for Determining Bactericidal Activity of Antimicrobial Agents; Approved*
576 *Guideline* (Vol. 19).
577 Orlandini, S., Pinzauti, S., & Furlanetto, S. (2013). Application of quality by design to the
578 development of analytical separation methods. *Analytical and Bioanalytical Chemistry*, *405*,
579 443–450. https://doi.org/10.1007/s00216-012-6302-2
580 Otoni, C. G., Espitia, P. J. P., Avena-Bustillos, R. J., & McHugh, T. H. (2016). Trends in
581 antimicrobial food packaging systems: Emitting sachets and absorbent pads. *Food Research*
582 *International*, *83*, 60–73. https://doi.org/10.1016/j.foodres.2016.02.018
583 Petriccione, M., De Sanctis, F., Pasquariello, M. S., Mastrobuoni, F., Rega, P., Scortichini, M., &
584 Mencarelli, F. (2015). The Effect of Chitosan Coating on the Quality and Nutraceutical Traits
585 of Sweet Cherry During Postharvest Life. *Food and Bioprocess Technology*, *8*, 394–408.
586 https://doi.org/10.1007/s11947-014-1411-x
587 Reddy, L. S., Babu, N. J., & Nangia, A. (2006). Carboxamide-pyridine N-oxide heterosynthon for
588 crystal engineering and pharmaceutical cocrystals. *Chemical Communications*, *13*, 1369–1371.
589 https://doi.org/10.1039/b515510j
590 Regulation (EC) No 1333/2008 of the European Parliament and of the Council of 16 December
591 2008 on food additives. (2008). In *Official Journal of the European Union*. Retrieved from
592 https://eur-lex.europa.eu/eli/reg/2008/1333/oj
593 Requena, R., Vargas, M., & Chiralt, A. (2019). Eugenol and carvacrol migration from PHBV films
594 and antibacterial action in different food matrices. *Food Chemistry*, *277*, 38–45.
595 https://doi.org/10.1016/j.foodchem.2018.10.093
596 Ribeiro-Santos, R., Andrade, M., Melo, N. R. de, & Sanches-Silva, A. (2017). Use of essential oils
597 in active food packaging: Recent advances and future trends. *Trends in Food Science and*
598 *Technology*, *61*, 132–140. https://doi.org/10.1016/j.tifs.2016.11.021
599 Stenmarck, Å., Jensen, C., Quested, T., & Moates, G. (2016). Estimates of European food waste
600 levels. In *FUSIONS*. Retrieved from https://www.eu-

fusions.org/phocadownload/Publications/Estimates of European food waste levels.pdf

Tyagi, A. K., & Malik, A. (2011). Antimicrobial potential and chemical composition of Eucalyptus globulus oil in liquid and vapour phase against food spoilage microorganisms. *Food Chemistry*, *126*, 228–235. https://doi.org/10.1016/j.foodchem.2010.11.002

UNI EN ISO 4833-1:2013. Microbiology of the food chain -- Horizontal method for the enumeration of microorganisms Colony count at 30 degrees C by the pour plate technique

Wieczyńska, J., & Cavoski, I. (2018). Antimicrobial, antioxidant and sensory features of eugenol, carvacrol and trans-anethole in active packaging for organic ready-to-eat iceberg lettuce. *Food Chemistry*, *259*, 251–260. https://doi.org/10.1016/j.foodchem.2018.03.137

Wiegand, I., Hilpert, K., & Hancock, R. E. W. (2008). Agar and broth dilution methods to determine the minimal inhibitory concentration (MIC) of antimicrobial substances. *Nature Protocols*, *3*, 163–175. https://doi.org/10.1038/nprot.2007.521

Wu, Z., Zhou, W., Pang, C., Deng, W., Xu, C., & Wang, X. (2019). Multifunctional chitosan-based coating with liposomes containing laurel essential oils and nanosilver for pork preservation. *Food Chemistry*, *295*, 16–25. https://doi.org/10.1016/j.foodchem.2019.05.114

Yildirim, S., Röcker, B., Pettersen, M. K., Nilsen-Nygaard, J., Ayhan, Z., Rutkaite, R., … Coma, V. (2018). Active Packaging Applications for Food. *Comprehensive Reviews in Food Science and Food Safety*, *17*, 165–199. https://doi.org/10.1111/1541-4337.12322

Table 1

Minimum inhibitory concentration (median and mean absolute deviation around the median-MADMe) expressed in µg/mL of the active compounds of EOs on the examined strains

	Cinnamaldehyde		Eugenol		Thymol		Carvacrol	
Strain	MIC	MADMe	MIC	MADMe	MIC	MADMe	MIC	MADMe
E. coli	256	43	1024	0	256	57	256	28
S.Typhimurium	512	0	>1024	n.d.	512	85	512	85
S. aureus	256	28	1024	0	256	85	512	57
MR *S. aureus*	256	0	1024	0	1024	256	256	0

n.d.: not determined

Table 2

Melting point of: coformers, active components of EOs and cocrystals

Compound	Melting point °C
HMT	280.0
INA	156.0
4HBA	215.5
THY	49.0
CAR	1.0
CIN	-7.5
HMT-THY	40.0
INA-CAR	63.7
4HBA-CIN	81.7

662

663 **Figure Captions**

664

665 **Fig. 1.** Antimicrobial activity of CIN, TYM and CAR against *Escherichia coli, Salmonella*
666 *Typhimurium, Staphylococcus aureus* and MR *Staphylococcus aureus* (n=3).

667

668 **Fig. 2.** Contour plots for absorbance units at 620 nm obtained plotting carvacrol concentration *vs.*
669 thymol concentration at 95 µg/mL cinnamaldehyde concentration.

670

671 **Fig. 3.** Probability map obtained plotting carvacrol concentration *vs.* thymol concentration at 105
672 µg/mL cinnamaldehyde concentration. The risk of having au responses > 0.05 is plotted.

673

674 **Fig. 4.** Release profile of the active components from pure EOs (solid line) *vs.* release profile of the
675 active components from the packaging prototypes (dashed line). Mean of triplicates.

676

677

678

679

680

681

682

683

Fig. 1.tiff

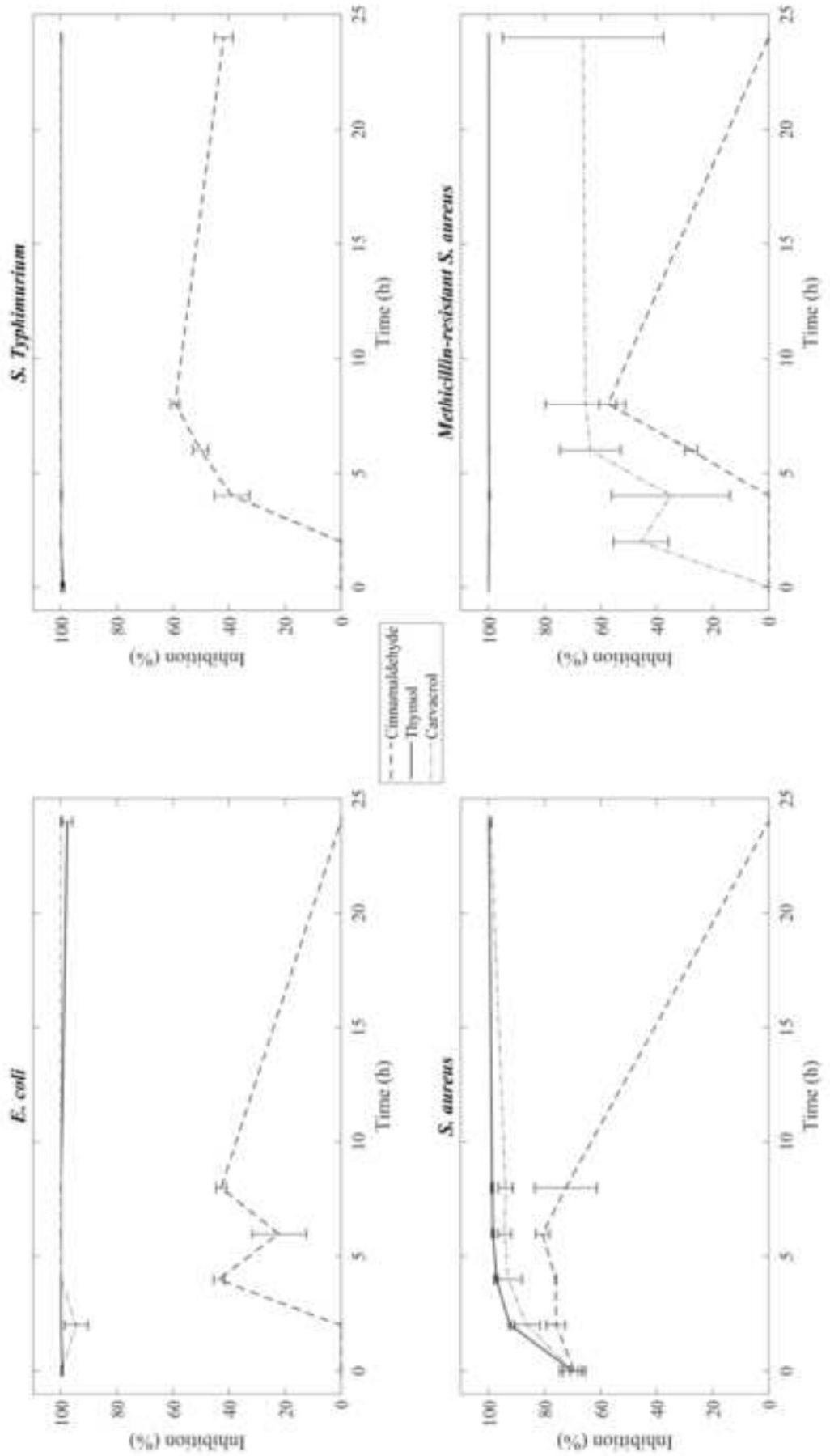

Figure 1
Click here to download high resolution image

Figure 2
Click here to download high resolution image

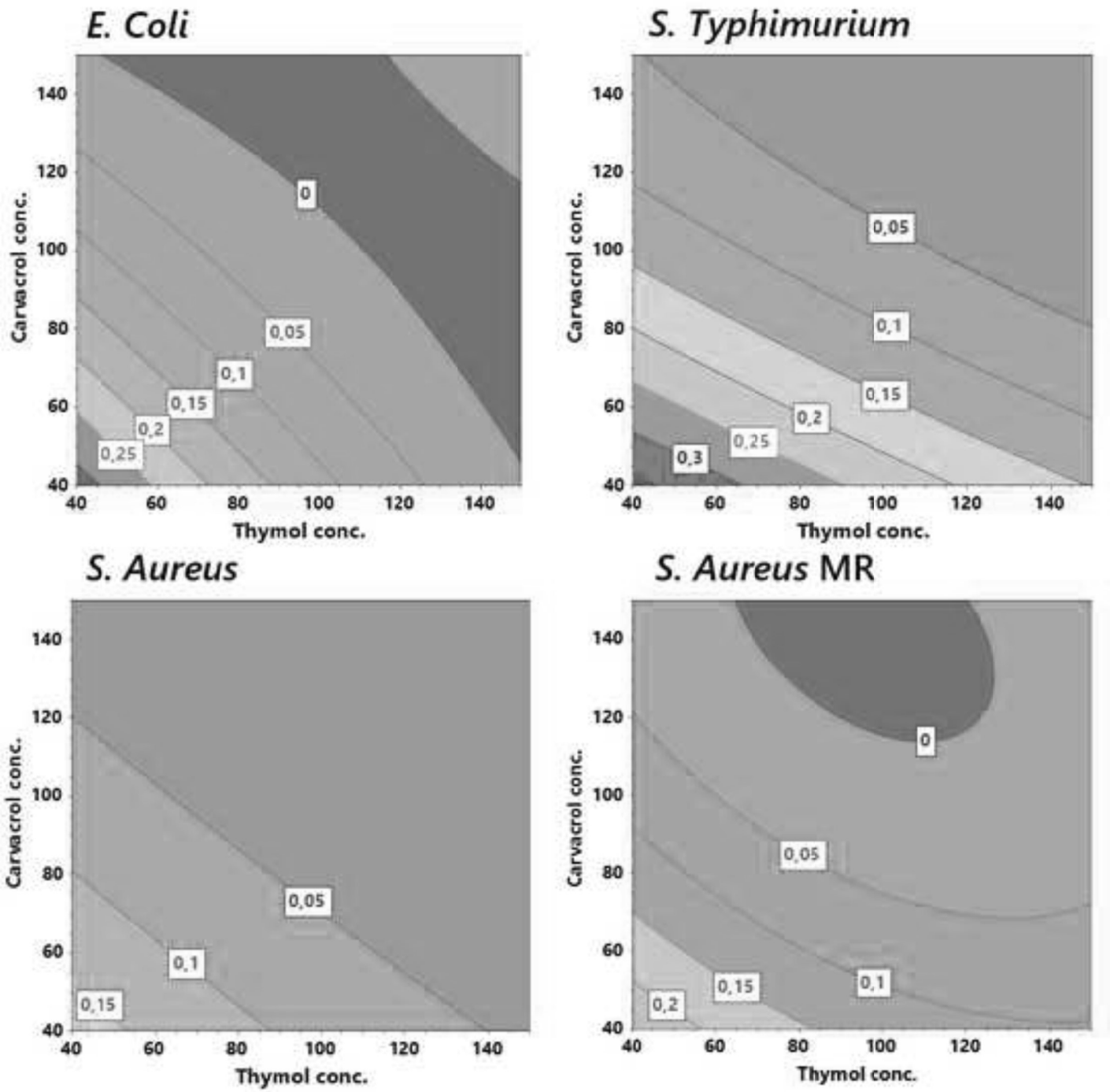

Livello

Livello incollato

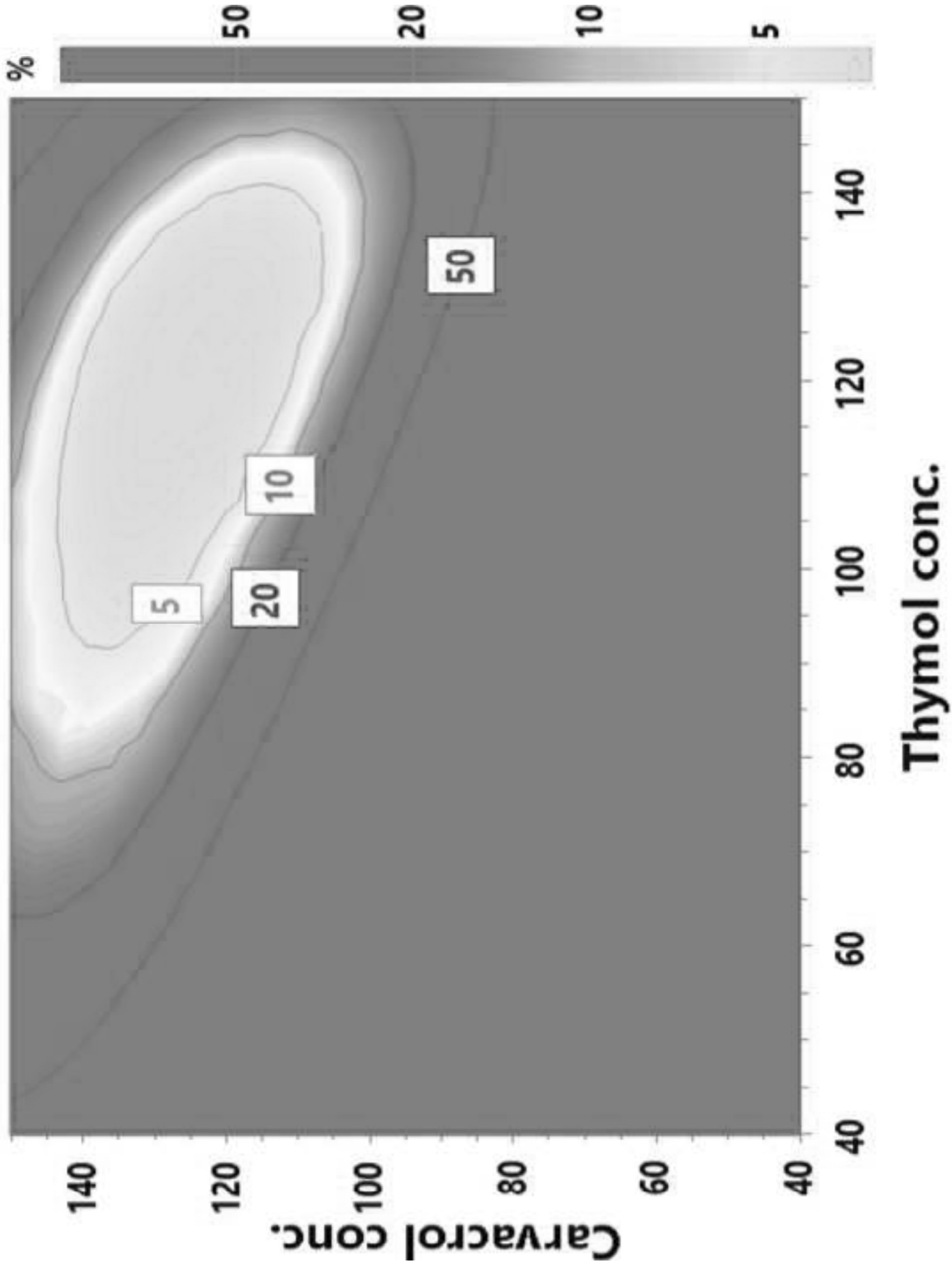

Figure 3
Click here to download high resolution image

Figure 4
Click here to download high resolution image